LEED structure analysis of the clean and (2×1)H covered Pd(110) surface

M. Skottke, R. J. Behm, and G. Ertl
Fritz Haber-Institut der Max Planck-Gesellschaft, D-1000 Berlin 33, Faradayweg 4-6, Federal Republic of Germany

V. Penka and W. Moritz
Institut für Kristallographie, Universität München, D-8000 München 2, Theresienstrasse 41, Federal Republic of Germany

(Received 19 February 1987; accepted 10 August 1987)

From an analysis of the low-energy electron diffraction (LEED) intensities we have determined the oscillatory distortion of the topmost interlayer spacings of the clean and the (2×1)H covered Pd(110) surface as well as the exact adsorption geometry in this latter structure, which is formed at $T < 180$ K at a coverage of $\theta_H \leqslant 1.0$. An R-factor analysis was used for quantitative comparison with the experimental data. The oscillatory distortion of the clean surface— $d_{12} = -5.1 \pm 1.5\%$, $d_{23} = +2.9 \pm 1.5\%$, d_{34} at its bulk value of 1.37 Å (with R factors $R_P = 0.22$, $R_{ZJ} = 0.14$)— is found to be reduced by the H adlayer to $d_{12} = -2.2 \pm 1.5\%$, $d_{23} = +2.9 \pm 1.5\%$, and d_{34} = bulk value. The H atoms are adsorbed on quasi-threefold sites with equal distances of 2.0 ± 0.1 Å to the two nearest Pd neighbors in the topmost and the closest Pd atom in the second layer, leading to an effective radius of the H atom of $r_H = 0.6 \pm 0.1$ Å. The long-bridge adsorption site, (octahedral) subsurface sites, or a hydrogen induced reconstruction via a lateral displacement of topmost Pd atoms by more than ± 0.1 Å can clearly be ruled out. These structural data, which are in good agreement with those of ordered H_{ad} structures on Ni(110) and Fe(110), characterize the (2×1)H structure on Pd(110) as being a typical adsorbate structure. There is no indication of either direct occupation of distinct subsurface or of near surface adsorption sites in this structure, nor does it open up channels for surface penetration, e.g., by a strong distortion of the topmost Pd substrate layers. In contrast to Ni(110) and Rh(110) the island growth of the (2×1)H structure on Pd(110) indicates predominantly attractive, indirect adatom–adatom interactions which, however, are of distinctly different nature than those causing island formation in the Pd–hydride phase.

I. INTRODUCTION

The most characteristic feature of palladium with respect to its interaction with hydrogen is its preeminent ability of hydrogen absorption leading to bulk dissolution at lower concentration (α-hydride) and the formation of a nonstoichiometric hydride (β-hydride, PdH_x) at higher concentration saturating at PdH. These phenomena in consequence were subject of a vast number of studies, an overview can be found in Ref. 1. Based on these results it has become clear that H adsorption can be regarded as a first step for its subsequent diffusion into the bulk. The exact mechanism for the onset of bulk diffusion of adsorbed hydrogen is not yet known, it has been shown that it can be enhanced by a surface reconstruction on Pd(110),[2–4] whereas on Pd(111) recent theoretical and experimental work led to the prediction of an easy and reversible transition of hydrogen atoms from adsorption sites into distinct subsurface sites and back,[5–8] followed by a slow, activated population of near surface absorption sites[9] as occupied on Pd(110).[2–4,10] The formation of subsurface hydrogen species as an intermediate step for diffusion into the bulk has been also proposed for H/Ru(001) by Yates *et al.*[11] A detailed investigation by VLEED (very low energy electron diffraction), however, showed no indication for the formation of subsurface layers.[12] Basic prerequisite for the further understanding of these processes is the exact knowledge of the hydrogen adsorption geometry on Pd surfaces, which in contrast to that of the bulk hydrides is so far unknown. We present here results of a LEED structure analysis of the (2×1)H structure on Pd(110) which also is the first example for a structure determination of an H/Pd-adsorption complex. Hydrogen adsorption on Pd(110) was first investigated at $T \geqslant 300$ K by Conrad *et al.*,[13] who reported the formation of a strongly disordered (1×2) structure indicated by streaked extra spots in the LEED pattern at the $[m, (2n+1)/2]$ positions. In a later LEED study extending the temperature range down to 130 K Behm *et al.* reported a (2×1) structure as an additional ordered phase,[2,3] which was confirmed by Rieder *et al.* using He diffraction.[4,10] This phase is characterized by missing diffraction beams at the $[(2n+1)/2,0]$ position at normal incidence, indicative of the existence of a glide symmetry plane in $[1\bar{1}0]$ direction and thus of a minimum concentration of two H_{ad} atoms per (2×1) unit cell. From the rather low intensities of the extra beams in the LEED pattern this structure was attributed to an ordered H adlayer, in contrast to a hydrogen induced reconstruction of the Pd substrate. Similar structures have equally been found on Ni(110)[14–16] while in none of the series of lattice gas structures on Rh(110) such a glide symmetry plane has been observed.[17] He-diffraction measurements with Ni(110)[14] and Pd(110)[4,10] led to the conclusion of a zig–zag arrange-

ment of the adsorbed H atoms on threefold coordinated sites along the close-packed metal rows in [1$\bar{1}$0] direction, in agreement with data from vibrational spectroscopy[18] and the results of semiempirical calculations.[19] A recent LEED analysis of the (2×1)H–Ni(110) finally could determine not only the nature of the adsorption sites but also the quantitative geometry of the adsorption complex including the distortions of the interlayer spacings between the first three substrate layers.[16] The finite probing depth of the low energy electrons[20]—in contrast to more surface sensitive techniques like He-beam diffraction—is not only responsible for the complexity of a LEED based structural analysis, but also allows to exactly determine the *entire* set of surface structural parameters. Based on the knowledge of these parameters not only the bonding geometry of the adsorbate is accessible, but also the adsorbate induced variation in the substrate structure can give valuable information concerning the substrate–adsorbate interaction and—in this context—about the transition from adsorption to bulk dissolution.

II. EXPERIMENTAL

The experiments were performed in a standard stainless steel UHV chamber with a base pressure of 1.5×10^{-10} Torr following bakeout, equipped with a four grid LEED optics, a cylindrical mirror analyzer for Auger electron spectroscopy (AES), a vibrating Kelvin probe for work function measurements ($\Delta\varphi$), and a quadrupole mass spectrometer for thermal desorption spectroscopy (TDS). Sample preparation consisted of repeated argon ion bombardment/annealing cycles until no further contaminants were detected by AES. Spurious amounts of carbon on the surface which are hardly detectable in AES due to the overlap of the C-*KLL* peak at 275 eV with the Pd-*MNN* peak at 282 eV, were reacted off by sequential heating cycles (900 K) with small amounts of coadsorbed oxygen.

The final cleanliness of the surface was judged from the shape of the H_2 TD spectra and the amount of the work function change during hydrogen adsorption [220 mV in the (2×1)H structure] both of which reacted very sensitively to small amounts of carbon contamination. The LEED intensities were collected by a computer interfaced Video system,[21] the angle of incidence was controlled and adjusted by comparing the intensity/voltage (I/V) curves of symmetrically equivalent beams. For oblique incidence this angle was determined by reflection of a laser beam to $\pm$ 1°, but in these calculations this angle has been tested as well. The final experimental data have been obtained by averaging the I/V spectra from equivalent beams.

The (2×1)H structure was produced by exposing the surface at 130 K to 0.3 L (1 L = 10^{-6} Torr s) H_2 which was determined from measurements of the coverage dependence in the (2×1)H related beams to represent the optimum coverage for this structure.[3] While at lower coverages the (2×1)H exists in islands, higher coverages cause a transition into the (reconstructed) (1×2) structure.[3] Due to the high sticking coefficient of H_2 on Pd(110) rapid measurements were required in order to avoid background adsorption of H_2 and slow conversion into the (1×2) structure. From the absence of any detectable intensity at the position of the (intense) beams of the (1×2) structure contributions from that structure could be ruled out.

III. CALCULATIONS

Before starting the intensity analysis for the adsorbate system we have investigated the clean surface. In that case the analysis is based on the comparison of 7 (9) nonequivalent beams at normal (off-normal) incidence within an energy range from 40 to 240 eV. The first three interlayer spacings were variable parameters [Fig. 1(c)]. On the hydrogen covered sample only one adsorption site—H adsorbed on quasi-threefold sites [Fig. 1(a)]—was tested following our experiences with the analogous Ni(110) system.[15] In that case a significant modification of the fractional order I/V curves resulted for H adsorbed on the long bridge sites[16] [Fig. 1(b)] which would lead to a significantly worse agreement also in the present case. Two data sets at off-normal incidence were used, one at $\theta = 7°$ and $\varphi = 0°$, the other at $\theta = 8.5°$ and $\varphi = 90°$. In total 3 (13) integral order and 1 (5) nonequivalent fractional order beams were used at normal (off-normal) incidence in an energy range of 40 to 180 eV. In this case the lateral (H_y) and vertical (H_z) displacement of the H atoms with respect to the topmost Pd atom represented two more variable parameters [Fig. 1(c)]. The reduced energy range was chosen because of the length of the computations on the one hand and the negligible intensity of the fractional order beams at higher energies on the other side. The reliability of the intensity analysis with a reduced energy range was tested on the clean Pd surface, evaluation of the I/V curves only in the 40 to 180 eV energy range did not affect the resulting structural parameters.

The LEED calculations itself were performed by using the layer doubling scheme to describe the interlayer multiple scattering.[22] For the adsorbate covered surface the topmost

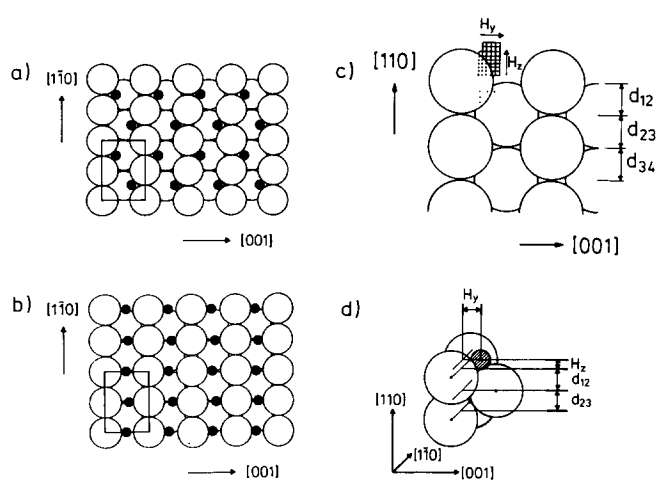

FIG. 1. Models of the (2×1)H–Pd(110) structure: (a) for H atoms on quasi-threefold sites, top view; (b) for H atoms on long-bridge sites, top view; (c) side view illustrating the structural parameters; (d) geometry of the local Pd_3–H adsorption complex.

layer of Pd atoms and the H atoms were treated as a combined layer.[22] Multiple scattering within this entity was calculated in angular momentum space, since for distances below ~0.7 Å between these layers this is more efficient. The number of angular momentum components as well as the number of atoms within the unit cell could be reduced by using symmetry adapted functions, since the summation over symmetrically equivalent positions in a unit cell can be performed prior to inversion of the matrix.[23]

Electron scattering by the Pd ion cores was described by up to eight phase shifts. Two different sets of phase shifts were used, one of them was obtained from a self-consistent band structure potential,[24] the other one was obtained from a superposition of relativistically calculated atomic potentials and the phase shifts were spin averaged.[25] Though in general the resulting intensities did not differ significantly, a few characteristic features [e.g., the 64 eV doublet in the (0,1) beam] could only be reproduced by using the latter set. In consequence all calculations reported here refer to those relativistic phase shifts. For the hydrogen atoms a muffin-tin potential was constructed from a fictitious H crystal with an atomic radius of 0.53 Å (1 a.u.) by symmetrizing the overlap between neighboring atoms. This approximation has previously been successfully applied in structural analyses of the H/Fe(110)[26] and the H/Ni(110)[16] systems. The real part of the inner potential was taken as constant to $V_{0r} = -10$ eV within the Pd and H layers. This value was found for the clean surface and is not corrected for work function differences between the surface and the LEED gun filament. An attempted fit to an energy dependent theoretical function by a procedure successfully tested on Cu(100)[27] did not yield a unique result. For the imaginary part we choose $V_{0i} = 0.85\ (E + V_{0r})^{1/3}$, thermal vibrations are accounted for by a Debye temperature of 274 K for all Pd and the H atoms. The effect of a reduced surface Debye temperature for the Pd atoms in the topmost layer ($\theta_s = 194$ K) was tested and found to be negligible. The agreement between experimental and calculated I/V curves is expressed in terms of R factors as introduced by Zanazzi and Jona (R_{ZJ})[28] and by Pendry (R_P).[29]

IV. RESULTS

For the clean surface the optimum structure was obtained with the third interlayer spacing, d_{34}, at its bulk value of 1.37 Å. The R-factor contour plots in Fig. 2 reflect the response of the R factors upon variation of d_{12} and d_{23}, with d_{34} at its bulk value. Both R factors reach their minima—$R_P = 0.22$ and $R_{ZJ} = 0.14$—at basically identical structures, defined by $d_{12} = 1.30$ Å and $d_{23} = 1.41$ Å. From a statistical analysis the error bars are estimated to ± 0.02 Å or $\pm 1.5\%$. Compared with the bulk interlayer separation we find an oscillatory distortion of the first two spacings by $-5.1 \pm 1.5\%$ and $+2.9 \pm 1.5\%$, respectively. The kind of agreement achieved is illustrated in Fig. 3 which depicts the experimental I/V data together with the "best model" of calculated I/V curves. The sensitivity of the I/V curves towards even relatively small structural changes is evident from the set of curves in Fig. 4. For each beam it demonstrates the effect of varying the topmost interlayer separation (upper triple from bottom to top: $d_{12} = 1.24$, 1.30, 1.37 Å) while d_{23} is kept constant at 1.40 Å and of varying d_{23} (lower triple from bottom to top: $d_{23} = 1.34$, 1.40, 1.47 Å) while $d_{12} = 1.30$ Å. The experimental data are included for comparison as the middle curve.

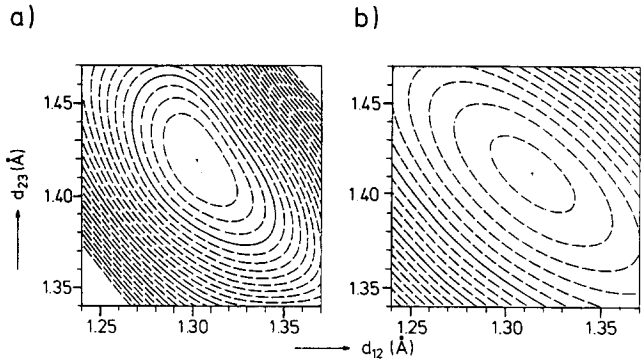

FIG. 2. (a) (Pendry) R-factor contour plot for the clean Pd(110) surface upon variation of d_{12} and d_{23} ($d_{34} = 1.37$ Å = bulk value) $0.22 < R_P < 0.47$; (b) (Zanazzi–Jona) R factor as in (a) $0.14 < R_{ZJ} < 0.34$.

For the adsorbate covered surface the analysis was split up into three steps. The calculated I/V curves of the integral order beams turned out to be rather insensitive with respect to the position of the H atoms, which had also been observed

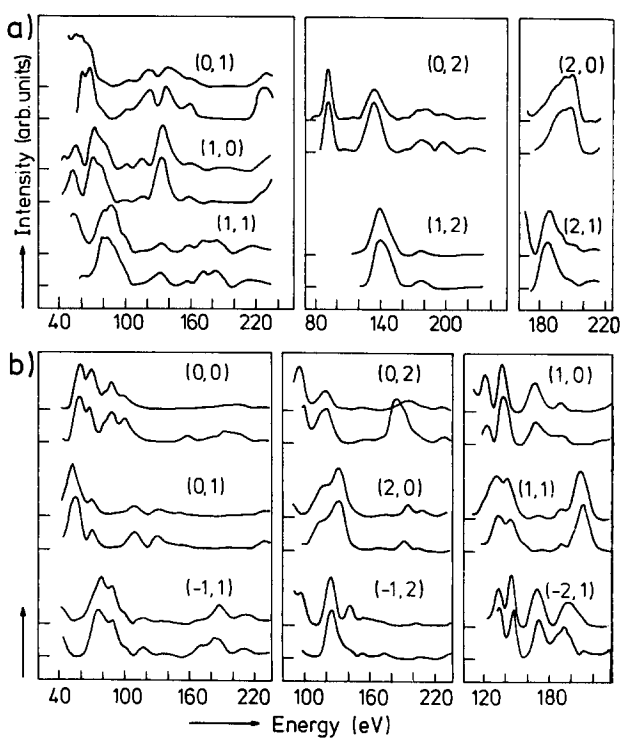

FIG. 3. Experimental (lower) and theoretical (upper) I/V curves calculated close to the best model of the clean Pd(110) surface ($d_{12} = 1.30$ Å, $d_{23} = 1.40$ Å, $d_{34} = 1.37$ Å = bulk value); (a) normal incidence; (b) off-normal incidence: $\theta = 7.0°$, $\varphi = 0.0°$.

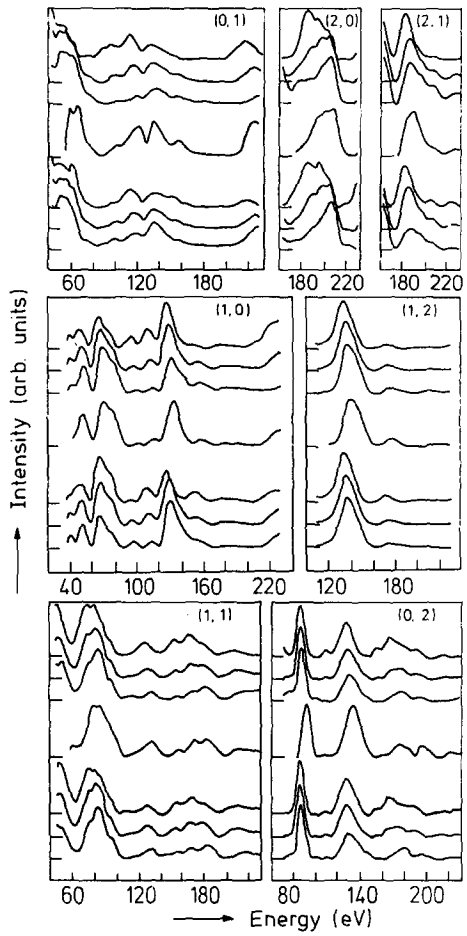

FIG. 4. Response of calculated I/V curves on Pd(110) upon variation of topmost (d_{12}) or second (d_{23}) interlayer spacing while the other respective one is kept constant. From bottom to top: $d_{12} = 1.30$ Å/$d_{23} = 1.34$ Å, 1.30 Å/1.40 Å, 1.30 Å/1.47 Å, experimental data, 1.24 Å/1.40 Å, 1.30 Å/1.40 Å, 1.37 Å/1.40 Å.

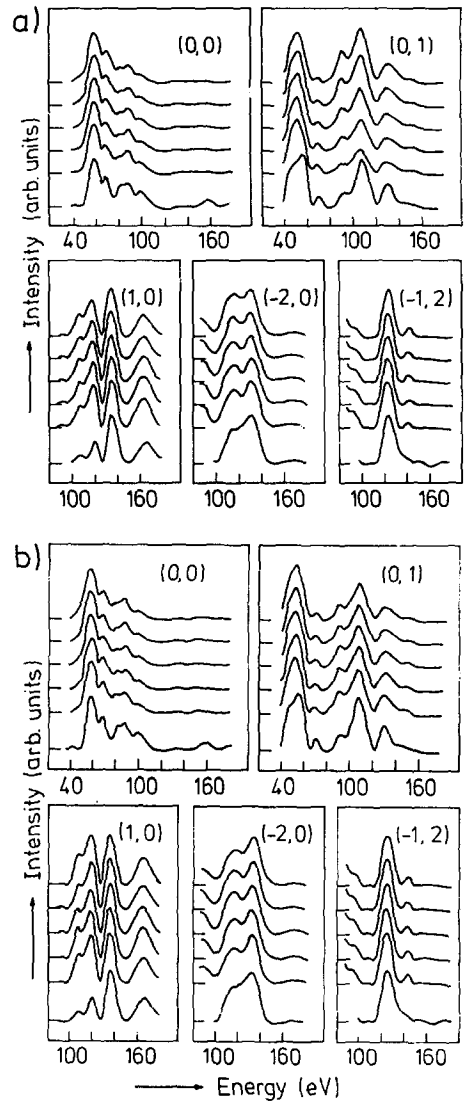

FIG. 5. Response of calculated I/V curves of the integral order beams upon variation of the lateral (H_y) or vertical (H_z) position of the H atoms while the other respective parameter and the Pd lattice ($d_{12} = 1.35$ Å, $d_{23} = 1.41$ Å) are kept constant (off-normal incidence). From bottom to top: (a) Experimental data, calculated curves with $H_z = 0.6$ Å, $H_y = 0.9$, 1.1, 1.3, 1.5, 1.7 Å; (b) experimental data, calculated curves with $H_y = 1.3$ Å, $H_z = 0.3$, 0.45, 0.60, 0.75, 0.90 Å.

for the ordered H_{ad} structures on Fe(110)[26] and Ni(110)[16] and which is due to the low scattering power of the H atoms (Fig. 5). Therefore the Pd–Pd interlayer spacings could be determined independently to a good approximation just from the integral order beams. In turn the position of the H atoms was determined from the I/V data of the fractional order beams only using the previously determined Pd–Pd interlayer spacings. Due to the relatively independent effects of the structural parameters of Pd and H atoms, respectively, the process of finding the minimum R factor in the multidimensional space has been simplified in this way. Finally all positions were optimized independently using the entire data set.

Figure 6(a) represents the response of the Pendry R factor, calculated over all beams at normal incidence, on the variation of d_{12} and d_{23} at a fixed position of the H atoms ($H_y = 1.3$ Å, $H_z = 0.6$ Å). The minimum of $R_P = 0.23$ for these beams is reached for $d_{12} = 1.34$ Å and $d_{23} = 1.40$ Å. In a separate analysis the minimum R factors for all beams at oblique incidence ($R_P = 0.37$, $R_{ZJ} = 0.19$) were obtained for $d_{12} = 1.34$ Å and $d_{23} = 1.41$ Å, almost identical to the above result on the data set at normal incidence. Compared to the clean surface the contraction of the topmost interlayer spacing is reduced from $-5.1 \pm 1.5\%$ to $-2.2 \pm 1.5\%$, while the relaxation of the second one $+2.9 \pm 1.5\%$ is not affected within the error limits of our analysis. The third interlayer spacing d_{34} remains at its bulk value.

Based on these structural parameters of the substrate the position of the H atoms was determined. Figure 7 shows I/V curves of extra beams calculated at constant Pd spacings close to their optimum values, $d_{12} = 1.35$ Å, $d_{23} = 1.41$ Å, while the position of the H atoms was varied. The range of H positions which was scanned systematically is indicated in Fig. 1(c). Test calculations for subsurface sites as shown in

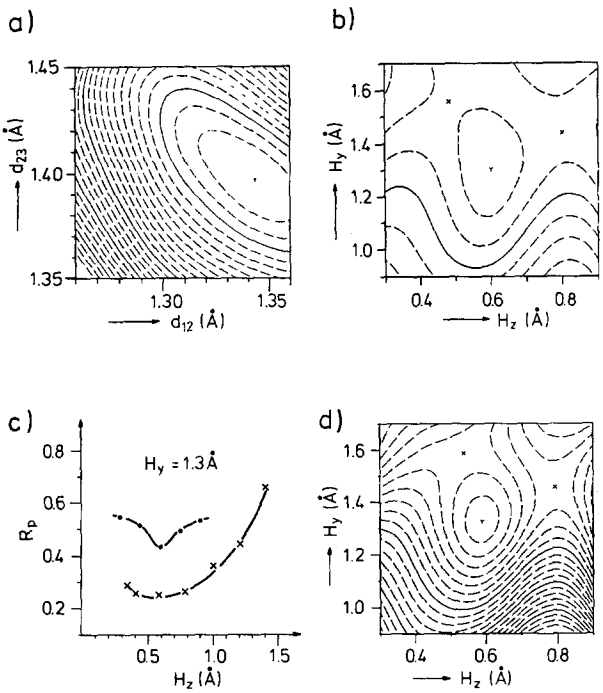

FIG. 6 (Pendry) R-factor dependence of the (2×1)H–Pd(110) structure upon variation of two structural parameters while the remaining ones are kept close or at their optimum value: (a) Contour plot of the R factor as a function of the first two Pd interlayer spacings ($H_y = 1.3$ Å, $H_z = 0.6$ Å) averaged over all beams at normal incidence ($0.23 < R_P < 0.48$); (b) contour plot of the R factor as a function of the position of the H atoms ($d_{12} = 1.35$ Å, $d_{23} = 1.41$ Å) averaged over all beams at off-normal incidence; (c) contour plot of the R factor as a function of the vertical position H_z of the adatom at a fixed lateral position $H_z = 1.3$ Å averaged over the fractional order beams only at $\theta = 8.5°$ $\varphi = 90°$ (upper curve) and at normal incidence (lower curve) [d_{12} and d_{23} as in (b)]; (d) as (b), but averaged only over all fractional order beams at oblique incidence.

Fig. 1(c) yielded a considerably worse agreement. Occupation of octahedral sites—on the long-bridge position as well as in subsurface position underneath the short bridge sites of the topmost layer of Pd atoms—can likewise be ruled out from symmetry reasons. Such structures do not exhibit the glide symmetry plane required by the LEED pattern. A contour plot of R_P (for all beams at off-normal incidence) as a function of H_y and H_z at fixed Pd interlayer spacings is reproduced in Fig. 6(b). The minimum values of $R_P = 0.37$ and $R_{ZJ} = 0.19$ result for an adatom position at $H_y = 1.3 \pm 0.1$ Å and $H_z = 0.6 \pm 0.1$ Å.

This is confirmed by a separate evaluation of the fractional order beams only which react more sensitively to the position of the H atoms. From Fig. 6(d) it becomes clear that there is no additional minimum at lower values of H_z. Higher values can be ruled out from the more extensive variation of H_z at one particular value of H_y–$H_y = 1.3$ Å—as shown in Fig. 6(c) for half-order beams at normal incidence (lower curve) and at $\theta = 8.5°$, $\varphi = 90°$ (upper curve).

If the y/z coordinates of the H atom are converted into Pd–H bond lengths to the three neighboring Pd atoms, nearly equal values of 2.0 ± 0.1 Å are obtained, i.e., the H atom is indeed adsorbed at a threefold site formed by two Pd atoms from the topmost layer and one Pd atom from the layer underneath [Fig. 1(d)]. Using the bulk value of 1.37 Å for the atomic radius of the Pd atoms we obtain 0.6 ± 0.1 Å for the effective radius of the H atoms.

In addition to these lattice-gas structures where the extra beams result solely from an ordered H adlayer also a hydrogen induced (2×1) reconstruction was tested. From symmetry arguments only an alternating lateral displacement of the topmost Pd atoms would be possible (Fig. 1). The relative intensity and the I/V profile of the fractional order beams calculated for a lateral displacement of Pd

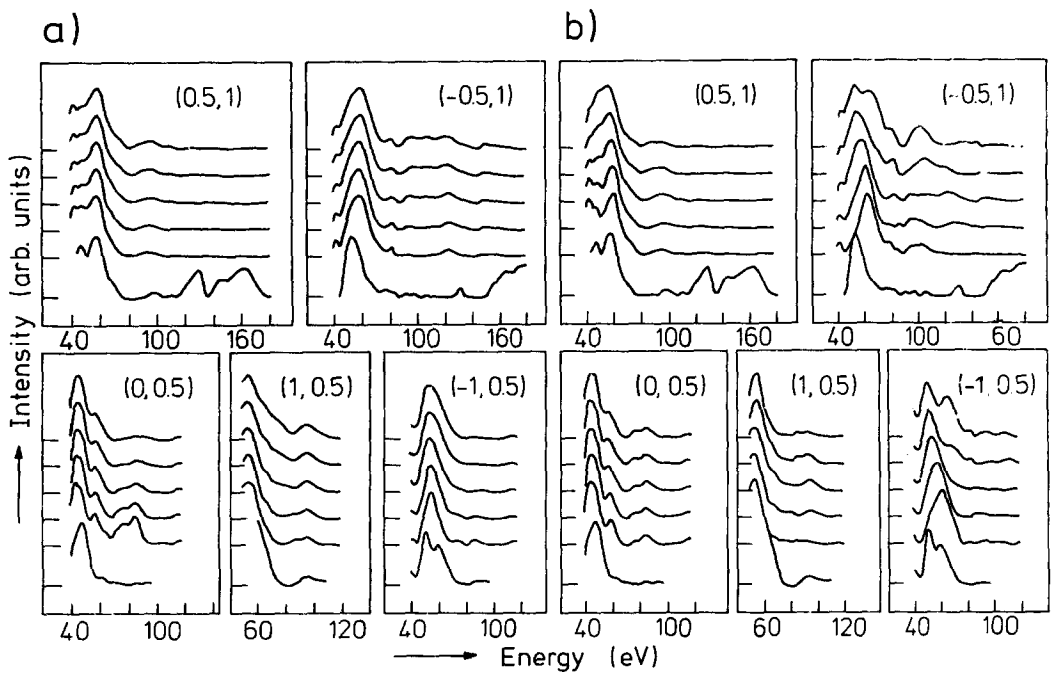

FIG. 7. Response of calculated I/V curves of the fractional order beams upon variation of the lateral (H_y) or vertical (H_z) position of the H atoms while the other respective parameter and the Pd lattice ($d_{12} = 1.35$ Å, $d_{23} = 1.41$ Å) are kept constant (off-normal incidence). From bottom to top: (a) experimental data, calculated data with $H_z = 0.6$ Å, $H_y = 0.9$, 1.1, 1.3, 1.5, 1.7 Å; (b) experimental data, calculated data with $H_y = 1.3$ Å, $H_z = 0.30$, 0.45, 0.60, 0.75, 0.90 Å.

atoms of ± 0.3 Å clearly rule out any such reconstruction involving more than 0.1 Å lateral displacement of the Pd atoms and thus confirm the assignment of the ordered H adlayer as the origin of the extra beams in the LEED pattern.

V. DISCUSSION

The structure of the clean Pd(110) very much resembles that of comparable fcc(110) surfaces which equally exhibit a oscillating distortion of the topmost interlayer spacing (Table I). This has been explained recently in a simple electrostatic model as a general surface effect, which, however, is most strongly present on "open" surfaces due to their smaller interlayer distance.[45] The structure obtained here is also in good agreement with results of a recent LEED structure analysis for the same surface by Barnes *et al.*, who determined these distortions to $-6 \pm 2\%$ for d_{12} and $+1 \pm 2\%$ for d_{23}.[40] From a technical point of view, it has also become clear that palladium is just at the verge of becoming a "high Z" material which requires the use of a relativistic scattering potential: A few features in the I/V curves could only be reproduced by using that kind of potential, in contrast, e.g., to our recent experience with nickel.[16,46]

Starting point for the discussion of the hydrogen covered surface is the comparability to other H_{ad}/fcc(110) systems or, taking the question around: Is there anything special in the structure of the adsorbed H adlayer on Pd(110) which could be correlated to the absorption properties of the H/Pd system? The formation of a (2×1)H superstructure has so far been reported for Ni(110)[14–16] and Pd(110)[2–4,10] and has also been interpreted theoretically in terms of a strong attraction between the H atoms within the zig–zag rows in $[1\bar{1}0]$ direction.[19] On Cu(110) in contrast only a disordered H adlayer has been found at temperatures down to 100 K.[39,47] A closer look reveals distinct differences within the systems exhibiting a (2×1)H superstructure: While on Ni(110) the (2×1)H structure is formed last in a whole series of lattice gas structures [for Ni(110) all seem to exhibit the zig–zag-line configuration],[14–17] with Pd(110) the (2×1)H structure is the only ordered overlayer structure and exhibits the characteristics of an island growth behavior, i.e., it can be attributed to predominantly attractive interactions within the H adatoms in that structure. Similar interactions between H adatoms have also been reported for H/Pd(100)[48] and one could speculate whether they originate from similar grounds as the attractive interactions between H atoms in neighbored octahedral sites in bulk palladium.[49] But in contrast to the indirect electronic interactions between H atoms on the surface the attraction between absorbed H atoms are attributed to an elastic deformation of the Pd lattice,[49] refuting this speculation.

The adsorption site itself also follows a tendency of small atoms like H_{ad} to adsorb in highly coordinated sites as equally been found for Fe(110),[26] Pt(111),[50] Ni(111),[51] Pd(100),[52] and Ni(100).[53] This strong tendency towards a high number of coordinating metal atoms at favorable distances might even cause the H atom to switch from a fourfold adsorption site on Pd(100) into a quasi-threefold site off-center, as predicted in recent calculations.[19] Embedded atom calculations for H/Pd(111) also revealed the threefold site to be most favorable, in those calculations, in addition, (threefold) subsurface sites were found to be equally favorable within the ordered $(\sqrt{3}\times\sqrt{3})R\,30°$ phase,[5,7] which could clearly be ruled out as an adsorption site for the present (2×1) structure on Pd(110). Calculations of the full adiabatic potential energy surface of the H/Ni(110) system, which were performed by Nordlander *et al.*[54] following the "effective medium" scheme[55] resulted in a very smooth potential along the troughs of the (110) surface with minima at the quasi-threefold and the long-bridge sites, respectively. The latter, however, can be clearly ruled out on the basis of the present analysis. If *single* H atoms were delocalized also on Pd(110), the indirect attractive interactions between neighbored adatoms across a metal atom would force them into localized adsorption sites.

The resulting local geometry of the Pd_3–H adsorption complex and the Pd–H distance of 2.0 ± 0.1 Å are very close to the structure of the stoichiometric Pd–β-hydride (NaCl-type lattice, Pd–H: 2.013 Å[56]). The atomic radius $r_H = 0.6 \pm 0.1$ Å is slightly larger than those reported in recent studies of H/Fe(110)[26] and H/Ni(110),[16] $r_H = 0.47 \pm 0.1$ Å. On Ni(111), in turn, where also threefold sites are occupied in the (2×2)H structure, a Ni–H bond length equivalent to $r_H = 0.6$ Å had been determined.[51] In view of the error limits associated with the results of the above LEED studies—caused by the rather weak effect of especially the lateral position H_y of the H atoms upon the LEED I/V curves—they are still considered to be in agreement with a basically uniform radius of the H_{ad} species rather than to reflect chemical differences between them. This interpretation is corroborated by the identical corrugation amplitudes of 0.26 Å measured by He diffraction on the (2×1)H structures on Pd(110)[4,10] and Ni(110).[14] Also the Ni–H distance for H atoms in (the octahedral holes of) Ni–hydride, Ni–

TABLE I. Oscillatory contraction of the topmost two interlayer separations d_{12} and d_{23} for clean and adsorbate covered fcc(110) surfaces.

Surface	d_{12}(%)	d_{23}(%)	References
Ni(110)	-8.4 ± 0.8	$+3.1 \pm 1.0$	31
	-9.8 ± 1.8	$+3.8 \pm 1.8$	32
	-8.7 ± 1.5	$+3.0 \pm 0.6$	33
	-8.5 ± 1.5	$+3.5 \pm 1.5$	16
Ni(110) + (2×1)H	-4.5 ± 1.5	$+5.0 \pm 1.5$	16
Ni(110) + c(2×2)S	+10.2	−3.2	34
Cu(110)	-8.2 ± 0.6	$+2.5 \pm 0.8$	35
	−8.5	+2.9	36
	−7.9	+2.4	37
	−5.3	+2.3	38
Cu(110) + "(1×1)"H	−0.8	+2.8	39
Pd(110)	-6.0 ± 2	$+1.0 \pm 2$	40
	-5.1 ± 1.5	$+2.9 \pm 1.5$	this work
Pd(110) + (2×1)H	-2.2 ± 1.5	$+2.9 \pm 1.5$	this work
Ag(110)	−5.7	+2.2	41
	−8.0	···	42
Al(110)	−8.6	+5.0	43
	−8.5	+5.5	44
Rh(110)	-7 ± 1	$+2 \pm 1$	30
Rh(110) + (1×1)H	-2 ± 1		30

H = 1.88 Å or $r_H = 0.63$ Å[57] falls into this range. The values calculated by Muscat[19] for H/Ni(110), $r_H = 0.39$ Å, and for H/Pd(110), $r_H = 0.43$ Å, are significantly lower and describe a hydrogen atom more similar to that in the $H_2Ni_4(C_5H_5)_4$ complex, which from its local geometry resembles H_{ad} on a threefold site ($r_H = 0.44$ Å).[58]

The adsorbate induced modification of the Pd surface also does not indicate any peculiarity. A (lateral) reconstruction of the lattice by more than 0.1 Å can clearly be ruled out. The changes in the oscillatory distortion of the interlayer spacings caused by the presence of the adsorbate very much resemble those found in other H adsorbate layers: Obviously the H adlayer tends to partially offset the distortion of these spacings caused by the surface truncation of the bulk and this effect is the more pronounced the larger the distortions are for the clean surface. For Fe(110) with no resolvable distortion on the clean surface, H_{ad} is also reported not to modify the substrate structure.[26] On Ni(110), Rh(110), and Cu(110) in contrast, which exhibit significant distortions in their clean state by $-8.5/+3.5$,[16] $-7/+2\%$,[30] and $-9.4/+4.9\%$,[39] the H adlayer causes significant changes towards a more bulk-like structure, namely to $-4.5/+5\%$,[16] $-2/\pm 0\%$,[30] and $-0.8/+2.8\%$.[39] It should be pointed out that in all these cases the first interlayer spacing is much more affected than the second one, as expected.

In the context of hydrogen adsorption these results can be interpreted in the way that the (2×1)H phase is by all structural standards characterized as a typical ordered overlayer. There is no structural evidence for any preformation of penetration paths for H atoms which might facilate dissolution. Such paths could be opened up, e.g., by a strong H induced deformation of the topmost Pd substrate layers or by the rapid population of subsurface sites even at low temperatures as proposed for H/Pd(111).[7] The present structure can rather serve as proof that for H/Pd(110) adsorption and absorption process can be strictly separated.[13,59]

The occupation of subsurface sites is apparently favored only by the hydrogen induced (1×2) reconstruction of the surface. The lattice distortion in this "row pairing" reconstruction,[60,61] which is equally well known also for Ni(110)[14,46] must be strong enough to open up channels for the subsequent population of distinct subsurface sites as well as for the onset of slowly filling absorption sites in the near-surface region.[2,10] At elevated temperatures $T > 200$ K the (2×1)H structure disorders and subsequently converts into (a poorly ordered) (1×2) reconstructed phase, the (2×1)H thus is metastable with respect to this latter structure, again closely resembling the behavior of Ni(110).[62,63] At these higher temperatures the process of bulk dissolution is fast enough to effectively compete with the adsorption process under most experimental conditions.[59]

VI. CONCLUSIONS

In this LEED intensity analysis of the clean and (2×1)H covered Pd(110) surface we have confirmed that the H atoms occupy quasi-threefold adsorption sites, as suggested previously, and have determined the actual geometry of the local Pd_3–H adsorption complex: From the (reduced) oscillatory distortion of the topmost interlayer spacings d_{12}: $-5.1 \pm 1.5\%$ to $-2.2 \pm 1.5\%$, d_{23}: $+2.9 \pm 1.5\%$ to $+2.9 \pm 1.5\%$, d_{34} at its bulk value of 1.37 Å, and from the lateral (H_y) and vertical (H_z) displacement of the H atoms with respect to the topmost Pd atoms—$H_y = 1.3 \pm 0.1$ and $H_z = 0.6 \pm 0.1$ Å—the Pd–H distances turn out to be equal within the limits of accuracy, namely 2.0 ± 0.1 Å leading to an effective hydrogen radius of $r_H = 0.6 \pm 0.1$ Å. A hydrogen induced reconstruction of the lattice by a lateral displacement of topmost Pd atoms by more than 0.1 Å can be ruled out, the extra beams are caused by diffraction in the ordered H adlayer. This phase is characterized as a typical overlayer structure without any indication for the onset of surface penetration, e.g., by lattice distortion or occupation of subsurface sites/near surface absorption sites. The predominantly attractive, indirect adatom–adatom interaction leading to this structure are of distinctly different nature than the attractive interaction between neighbored adsorbed H atoms in the hydride phase, which are attributed to an elastic lattice deformation.

ACKNOWLEDGMENT

Financial support by the Deutsche Forschungsgemeinschaft (SFB 128) is gratefully acknowledged.

[1] *Hydrogen in Metals I and II*, Topics in Applied Physics Vols. 28–29, edited by G. Alefeld and J. Völkl (Springer, Berlin, 1978).
[2] R. J. Behm, V. Penka, M. G. Cattania, K. Christmann, and G. Ertl, J. Chem. Phys. **78**, 7486 (1983).
[3] M. G. Cattania, V. Penka, R. J. Behm, K. Christmann, and G. Ertl, Surf. Sci. **126**, 382 (1983).
[4] M. Baumberger, W. Stocker, and K. H. Rieder, Appl. Phys. A **41**, 151 (1986).
[5] S. M. Foiles and M. S. Daw, J. Vac. Sci. Technol. A **3**, 1565 (1985).
[6] T. E. Felter and R. H. Stulen, J. Vac. Sci. Technol. A **3**, 1566 (1985); R. H. Stulen and G. D. Kubiak, *ibid.* **4**, 1427 (1986).
[7] T. E. Felter, S. M. Foiles, M. S. Daw, and R. H. Stulen, Surf. Sci. **171**, L379 (1986).
[8] M. S. Daw and S. M. Foiles, Phys. Rev. B **35**, 2128 (1987).
[9] G. E. Gdowski, R. H. Stulen, and T. E. Felter, J. Vac. Sci. Technol. A **5**, 1103 (1987).
[10] K. H. Rieder, M. Baumberger, and W. Stocker, Phys. Rev. Lett. **51**, 1799 (1983).
[11] J. T. Yates Jr., C. H. F. Peden, J. E. Houston, and D. W. Goodman, Surf. Sci. **160**, 37 (1985).
[12] P. Feulner, H. Pfnür, P. Hofmann, and D. Menzel, Surf. Sci. **173**, L576 (1986).
[13] H. Conrad, G. Ertl, and E. E. Latta, Surf. Sci. **41**, 435 (1974).
[14] K. H. Rieder and T. Engel, Phys. Rev. Lett. **43**, 373 (1979); **45**, 824 (1980); Surf. Sci. **164**, 55 (1985).
[15] V. Penka, K. Christmann, and G. Ertl, Surf. Sci. **136**, 307 (1984).
[16] W. Reimer, V. Penka, M. Skottke, R. J. Behm, and G. Ertl, Surf. Sci. **186**, 45 (1987).
[17] K. Christmann, M. Ehsasi, W. Hirschwald, and J. H. Block, Chem. Phys. Lett. **131**, 192 (1986).
[18] N. J. DiNardo and E. W. Plummer, Surf. Sci. **150**, 89 (1985), and references therein.
[19] J. P. Muscat, Surf. Sci. **110**, 389 (1981); M. S. Daw and S. M. Foiles, in *The Structure of Surfaces*, edited by M. A. van Hove and S. Y. Tong (Springer, Berlin, 1984).
[20] G. Ertl and J. Küppers, *Low Energy Electrons and Surface Chemistry* (Verlag Chemie, Weinheim, 1985).
[21] E. Lang, P. Heilmann, G. Hanke, K. Heinz, and K. Müller, Appl. Phys. **19**, 7 (1979).
[22] J. B. Pendry, *Low Energy Electron Diffraction* (Academic, London, 1974).
[23] W. Moritz, J. Phys. C **17**, 353 (1984).
[24] V. L. Moruzzi, J. F. Janak, and A. R. Williams, *Calculated Electronic*

Properties of Metals (Pergamon, New York, 1978).
[25]R. Feder and W. Moritz, Surf. Sci. **77**, 505 (1978).
[26]W. Moritz, R. Imbihl, R. J. Behm, G. Ertl, and T. Matsushima, J. Chem. Phys. **83**, 1959 (1985).
[27]W. Hösler, W. Moritz, R. Feder, and E. Tanum, Surf. Sci. **171**, 55 (1986).
[28]E. Zanazzi and F. Jona, Surf. Sci. **62**, 61 (1977).
[29]J. B. Pendry, J. Phys. C **13**, 937 (1980).
[30]K. Müller and K. Heinz (personal communication).
[31]Y. Gauthier, R. Baudoing, Y. Joly, C. Gaubert, and J. Rundgren, J. Phys. C **14**, 4547 (1984).
[32]M. L. Xu and S. Y. Tong, Phys. Rev. B **31**, 6332 (1985).
[33]D. L. Adams, L. E. Petersen, and C. S. Sørensen, J. Phys. C **18**, 1753 (1985).
[34]R. Baudoing, Y. Gauthier, and Y. Joly, J. Phys. C **18**, 4061 (1985).
[35]D. L. Adams, H. B. Nielsen, J. N. Andersen, I. Stensgaard, R. Feidenhans'l, and J. E. Sørensen, Phys. Rev. Lett. **49**, 669 (1982).
[36]D. L. Adams, H. B. Nielsen, and J. N. Andersen, Surf. Sci. **128**, 294 (1983).
[37]H. L. Davies and J. R. Noonan, Surf. Sci. **126**, 245 (1983).
[38]I. Stensgaard, R. Feidenhans'l, and J. E. Sørensen, Surf. Sci. **128**, 281 (1983).
[39]A. P. Baddorf, I. W. Lyo, E. W. Plummer, and H. L. Davies, J. Vac. Sci. Technol. A **5**, 782 (1987).
[40]C. J. Barnes, M. Q. Ding, M. Lindroos, R. D. Diehl, and D. A. King, Surf. Sci. **162**, 59 (1985).
[41]J. R. Noonan and H. L. Davies, Surf. Sci. **115**, L75 (1982).
[42]M. Alff and W. Moritz, Surf. Sci. **80**, 24 (1979).
[43]J. N. Andersen, H. B. Nielsen, L. Petersen, and D. L. Adams, J. Phys. C **17**, 173 (1984).
[44]J. R. Noonan and H. L. Davies, Phys. Rev. B **29**, 4349 (1984).
[45]K. M. Ho and K. P. Bohnen, Phys. Rev. Lett. **56**, 934 (1986).
[46]G. Kleinle, V. Penka, R. J. Behm, G. Ertl, and W. Moritz, Phys. Rev. Lett. **57**, 148 (1987).
[47]K. H. Rieder and W. Stocker, Phys. Rev. Lett. **57**, 2548 (1986).
[48]R. J. Behm, K. Christmann, and G. Ertl, Surf. Sci. **99**, 320 (1980).
[49]H. Brodowsky, Z. Phys. Chem. N.F. **44**, 129 (1965).
[50]A. M. Baró, H. Ibach, and D. Bruchmann, Surf. Sci. **130**, 1 (1983).
[51]K. Christmann, R. J. Behm, G. Ertl, M. A. van Hove, and W. H. Weinberg, J. Chem. Phys. **70**, 4168 (1979).
[52]C. Nyberg and C. G. Tengstal, Surf. Sci. **126**, 163 (1983).
[53]S. Anderson, Chem. Phys. Lett. **55**, 185 (1979).
[54]D. Nordlander, S. Holloway, and J. K. Nørskov, Surf. Sci. **136**, 59 (1984).
[55]J. K. Nørskov, Phys. Rev. Lett. **48**, 1620 (1982).
[56]A. C. Switendick, in Ref. 1.
[57]E. O. Wollau, J. W. Cable, and W. C. Koehler, J. Phys. Chem. Solids **24**, 1141 (1963).
[58]T. F. Koetzle, R. K. McMullan, R. Bau, D. W. Hart, D. L. Tipton, and R. D. Wilson, Adv. Chem. **167**, 61 (1978).
[59]T. Engel and H. Kuipers, Surf. Sci. **90**, 162 (1979).
[60]H. Niehus, C. Hiller, and G. Comsa, Surf. Sci. **173**, L599 (1986).
[61]W. Moritz, R. J. Behm, G. Ertl, G. Kleinle, V. Penka, W. Reimer, and M. Skottke, Surf. Sci. (in press).
[62]R. J. Behm, V. Penka, K. Christmann, G. Ertl, and R. J. Schwankner, in *The Structure of Surfaces*, edited by M. A. van Hove and S. Y. Tong (Springer, Berlin, 1984).
[63]K. Christmann, V. Penka, R. J. Behm, F. Chehab, and G. Ertl, Solid State Commun. **51**, 487 (1984).